## Title

Feedback Control for Natural Oscillations of Locomotion Systems Under Continuous Interactions With Environment



## Journal

IEEE Transactions on Control Systems Technology, 23(4)

## ISSN

1063-6536

## Authors

Chen, Zhiyong
Iwasaki, Tetsuya
Zhu, Lijun

## Publication Date

2015

## DOI

10.1109/tcst.2014.2363432

# Feedback Control for Natural Oscillations of Locomotion Systems Under Continuous Interactions with Environment

Zhiyong Chen, Tetsuya Iwasaki, and Lijun Zhu

***Abstract*—We consider a class of multi-body robotic systems inspired by dynamics of animal locomotion such as swimming and crawling. Distinctive properties of such systems are that the stiffness matrix is asymmetric due to skewed restoring force from the environment, and the damping matrix is a scalar multiple of the inertia matrix when the body is flat like those of fish. Extending the standard notion to this class, we define the natural oscillation as a free response under the damping compensation to yield marginal stability. The natural oscillation of the body provides a basic gait for locomotion. We propose a class of simple nonlinear feedback controllers to achieve entrainment to the natural oscillation of the body, resulting in a prescribed average velocity. As an example, a link chain system with symmetric mechanical structure is considered, and its natural oscillation is shown to exhibit traveling waves appropriate for undulatory locomotion. Controllers are designed under various conditions to achieve prescribed locomotion speeds by natural oscillations. In particular, it is shown how design parameters can be chosen to increase the rate of convergence, and how the locomotion speed can be set by adjusting the natural frequency through body stiffness compensation.**

***Index Terms*—Oscillations, locomotion, robotics, neuronal control, autonomous vehicles**

## I. Introduction

Propulsion mechanisms for transportation machines have been mostly based on rotating components such as wheels, screws, and propellers. On the other hand, animal/human locomotion has provided inspirations for new propulsion mechanisms for mobile robots that exploit dynamic interactions of periodic body movements with the surrounding environment [1]–[8]. Such mechanisms would allow robust and adaptive locomotion in rugged and changing environments. Fundamental problems in controlling robotic locomotion systems include how to determine an appropriate oscillation profile (frequency, amplitudes, and phases) of multiple motion variables, and how to achieve a prescribed oscillation profile as a stable limit cycle of the closed-loop system through feedback control.

Nonlinear oscillator theories have a long history and various analysis methods have been developed in the literature, including the Poincaré-Bendixson theorem [9], [10], Hopf bifurcation theorem [11], [12], perturbation theory and averaging [13], [14], the Malkin theorem for phase coupled oscillators [15]–[18], harmonic balance [19], [20], and the contraction analysis for global convergence [21]–[23]. Most of the results so far have focused on the analysis of limit cycles to prove existence, assess stability, and estimate frequency and amplitude, and there are very few general theories for the feedback control design of limit cycles. Recent work by Shiriaev *et al.* [24], [25] has developed one of such design theories. They considered stabilization of a periodic orbit for multiple degree-of-freedom (DOF), underactuated Euler-Lagrange systems. The virtual constraint approach was proposed to reduce the problem to that of a planar (two dimensional) system with an integral of motion. A sufficient condition was given for the existence of periodic solutions, but the problem of setting a desired oscillation profile has not been addressed.

Phase coordination of oscillating motion variables at a right frequency is important in achieving efficient locomotion. It is conjectured that the energy consumption during animal locomotion is minimized by exploiting the mechanical resonance between the body and the surrounding environment [26]–[28]. The idea of resonance, or natural oscillation, will be useful for designing efficient robotic locomotors that are robust against and adaptive to environmental changes. Feedback control laws to achieve entrainment to a resonance have been studied for single-DOF [29]–[35] as well as multi-DOF systems [36]–[39]. All of these work considered standard mechanical systems[1] for which natural oscillations are well defined. On the other hand, linearized dynamics of locomotion systems have asymmetric stiffness [40] arising from anisotropic environmental forces [4], [41], which prevents us from applying the standard definition of natural oscillations to locomotion systems.

In this paper, we shall first extend the notion of natural oscillations to the class of mechanical systems with asymmetric stiffness. The key idea is to consider the situation where the mechanical body is dragged by an external force at a constant velocity relative to the environment. For instance, one can imagine an eel placed in a constant flow of water with its head fixed to the inertial frame. At a nominal velocity commonly observed in biology, the eel body would be aligned with the flow, and the straight body configuration is the stable

Z. Chen and L. Zhu are with the School of Electrical Engineering and Computer Science, University of Newcastle, Callaghan, NSW 2308, Australia (zhiyong.chen@newcastle.edu.au, lijun.zhu@uon.edu.au). T. Iwasaki is with the Department of Mechanical and Aerospace Engineering, University of California, Los Angeles, CA 90095, USA (tiwasaki@ucla.edu). Z.Chen is the corresponding author.

The first author was supported by the Australian Research Council under Grant No.DP130103039. The second author was supported by the National Science Foundation under No.1068997, and by the Office of Naval Research, under MURI Grant N00014-08-1-0642.

[1]By standard mechanical systems, we mean those whose linearizations are described by symmetric positive definite mass, stiffness, and damping matrices.

equilibrium. However, if the damping effect is reduced by a proper amount, the system becomes marginally stable, thereby defining a natural oscillation similar to observed undulation. We will formalize this idea to define a natural oscillation in a general setting and show that the natural oscillation can be analytically characterized in terms of a generalized eigenvalue of the mass-stiffness matrix pair.

Once natural oscillation is defined, we will develop a rigorous method for designing a nonlinear feedback controller to achieve locomotion as a stable limit cycle of the closed-loop system, exploiting the natural dynamics of the open-loop plant. In the literature, locomotion control problems have been addressed for individual robotic systems [3], [42]–[46], but very few results are available to provide unified and effective theoretical tools for control design in a general setting. In this paper, we propose a simple control scheme by restricting the scope to the class of mechanical systems with asymmetric stiffness. This class of systems is fairly general to include arbitrary multibody robotic systems under continuous interactions with the environment, encompassing swimming and crawling [40], although it excludes systems with piecewise continuous dynamics with impacts, arising in legged locomotion. We use a simplified plant model obtained by assuming small body deformation around a nominal posture and by retaining up to the second order terms in the Taylor series. The proposed controller, based on nonlinear damping compensation and feedback linearization, achieves the natural oscillation with a guaranteed convergence for the simplified plant (all proofs are placed in Appendix). A design example for a link-chain locomotor will be given to illustrate the control method, with a validation through simulation of the original fully nonlinear model.

Some results of the present paper, in their preliminary forms, have been presented at conferences [47]–[49]. The first work on this topic appeared in [47], and was refined in [48], where the entrainment controller was designed based on the multivariable harmonic balance (MHB) analysis [50]. The MHB method allows us to develop tractable design conditions in a rather general setting, but existence and stability of the limit cycle prescribed for the closed-loop system are not guaranteed due to harmonic approximations. Later, we found a new approach for control synthesis to achieve exact entrainment to the natural oscillation [49]. The result in [49] considers the linear time-invariant plant dynamics under a fixed locomotion velocity. The present paper generalizes the result to include the dynamics associated with varying locomotion velocity, and provides a fully rigorous analysis of the targeted limit cycle oscillation. Preliminary versions of the design example in Section V were briefly presented in [48], [49].

## II. Problem formulation for locomotion control

We use the following notation. For a complex vector $z$, we denote $Ze^{j\phi} := z$ to define $Z$ to be the diagonal matrix with $|z_i|$ on the $i^{\text{th}}$ diagonal entry, $\phi$ to be the vector with $\angle z_i$ in the $i^{\text{th}}$ entry, and $e^{j\phi}$ to be the vector with $e^{j\phi_i}$ stacked in a column. The notation $x + y = z$ for $x \in \mathbb{R}$ and $y, z \in \mathbb{R}^n$ means that $z_i = x + y_i$ for the $i^{\text{th}}$ entry. Functions are assumed to act elementwise; for instance, $\cos(x)$ for $x \in \mathbb{R}^n$ is the vector whose $i^{\text{th}}$ entry is $\cos(x_i)$. For a complex number $\lambda$, $\Re(\lambda)$ and $\Im(\lambda)$ denote the real and imaginary parts of $\lambda$, respectively.

### A. The class of mechanical systems with asymmetric stiffness

We consider a general class of multi-body mechanical systems placed in an environment [40]. Each body joint is flexible and is driven by actuators. The environmental forces are assumed to result from continual interactions between the body and the surrounding media, and are modeled by static functions of the relative velocity. This class of robotic locomotors includes those like crawling snakes and swimming fish, but excludes those like walking legged-animals. The equations of motion have been developed in [40] using the Euler-Lagrange method, and are described by nonlinear differential equations in terms of motion variables for the shape and orientation of the body $\theta \in \mathbb{R}^m$, and for the locomotion velocity $v \in \mathbb{R}^k$.

We consider "cruising locomotion" of the robotic system and approximate the original nonlinear equations of motion in the neighborhood of this operating condition [40]. In particular, we assume symmetric body oscillations with small amplitudes around a nominal posture. By symmetry of oscillations, the direction of locomotion and body orientation can be constrained, reducing the dimension of $\theta$ to $n < m$ and that of $v$ from $k = 3$ to $k = 1$. The small amplitude assumption makes it reasonable to approximate nonlinearities by the Taylor series with truncation of higher order terms. As a result, the locomotor dynamics can be described by

$$J\ddot{\theta} + D\dot{\theta} + K(v)\theta = u \quad (1)$$

$$\dot{v} + \xi(\theta)v + \varphi(\theta, \dot{\theta}, \ddot{\theta}) = 0, \quad (2)$$

where $u \in \mathbb{R}^n$ is the actuator force/torque input, $\theta \in \mathbb{R}^n$ is the body shape variable, and $v \in \mathbb{R}$ is the locomotion velocity of the body (e.g., the center of gravity or the head). The $n \times n$ matrices $J$, $D$, and $K(v)$ represent the moment of inertia, damping, and velocity-dependent stiffness, respectively. The first equation shows how the change in the body shape $\theta$ results from actuation $u$ through the interaction with environment (represented by the dependence of $K$ on $v$). The second equation shows how a periodic change in the body shape $\theta$ is rectified to yield a biased forward velocity $v$. Throughout the paper, we call equations (1) and (2) an oscillation equation and a rectifier equation, respectively.

The simplified model is still nonlinear. We did not linearize the original model because linearization leads to decoupling of the two equations, losing the essential dynamics underlying thrust generation for locomotion. Thus, keeping up to the second order terms in the Taylor series, (1) and (2) represent one of the simplest models for locomotion systems. The simple model is obtained by restricting our attention to locomotion along a straight line with a symmetric body oscillation, and assuming that the oscillation amplitudes are small. When the body oscillation involves large curvature, the model may not accurately predict the locomotion velocity. However, the model qualitatively captures the essential dynamics of locomotion

and is reasonably accurate for the range of oscillation amplitudes observed in animals. The model equations in (1) and (2) have been derived in a general 3-dimensional setting in [40] and validated for various example systems [40], [41], [51], [52].

The following properties are assumed for the model.

**Assumption 2.1:** Let $v_o$ be a fixed constant in a desired range of locomotion velocity.

(a) $J = J^\intercal > 0$.
(b) $D = \mu J$ for some $\mu \in \mathbb{R}$.
(c) All the eigenvalues of $M(v_o) := J^{-1}K(v_o)$ are simple and have positive real parts.
(d) The eigenvalue $\lambda$ of $M(v_o)$ that minimizes $\Im(\lambda)/\sqrt{\Re(\lambda)}$ is unique.
(e) The functions $\xi$ and $\varphi$ are continuous, and $\xi(\theta)$ is positive for all nonzero $\theta$.

The model under this assumption captures a general robotic swimmer with a flat body, swimming at a low to moderate cruising speed, as explained below. The moment of inertia matrix $J$ for a general multi-body system is always symmetric positive definite as stated in (a). The Rayleigh damping $D = \mu J$ in (b) typically arises from modeling of slender-body fish (e.g. eels, saithe, rays) or their robotic counterpart, as a set of flat plates subject to resistive hydrodynamic forces [41], [51], [52]. In particular, the fluid force on a small plate segment is approximately modeled by a linear function of the plate velocity relative to the fluid, with its magnitude proportional to the plate area. Such model results in the fluid damping matrix $D$ proportional to the moment of inertia matrix $J$ with proportionality constant $\mu := c/\varrho$ where $c$ is the fluid drag coefficient and $\varrho$ is the body density. On the other hand, the stiffness matrix $K(v)$ is not necessarily symmetric due to the force from the environment. In particular, it is given by

$$K(v) = K_o + v\Lambda$$

where $K_o$ is a symmetric positive definite matrix representing the body stiffness, and $\Lambda$ is an asymmetric matrix representing the skewed stiffness arising from the locomotion at velocity $v$ relative to the environment [40]. We see that all the eigenvalues of $M(v)$ are real positive when $v = 0$ since $J$ and $K_o$ are positive definite. Hence, by continuity, there exists $\epsilon > 0$ such that the real parts of the eigenvalues of $M(v)$ are positive for all $|v| < \epsilon$. When the model represents animal locomotion, velocities typically observed in biology are well within this range [41], [53]. Thus, it seems reasonable to assume (c) for robotic locomotors. For simplicity, we introduced the additional assumption that no eigenvalues are repeated, which is generically satisfied. The item (d) is a technical assumption, which will turn out to give uniqueness of the natural oscillation. This assumption is always satisfied except for a very special case where there is a parabolic region $y^2 \leq cx$ with $c > 0$ on the complex plane $x + jy \in \mathbb{C}$, containing all the eigenvalues of $M(v)$ with more than one pair exactly on the boundary. Finally, item (e) is naturally satisfied by any physical locomotor system since the term $\xi(\theta)v$ in (2) represents the drag due to the environmental force.

### *B. Problem statements and overview of approach*

The ultimate goal is to develop a method for designing a feedback controller for the locomotor described by (1) and (2) such that efficient locomotion is achieved by exploiting a natural oscillation. With robotic applications in mind, our primary control target in this paper is not a precise regulation of position or velocity, but rather a robust maintenance of effective locomotion. We will define "natural oscillations" in a precise mathematical term, and develop a systematic method to achieve a natural oscillation with a theoretical guarantee for stability of the limit cycle. To this end, our approach is to break down the overall objective into the following two problems:

A. Define and characterize natural oscillations at velocity $v_o$ for the locomotion system described by (1) and (2).
B. Design a feedback controller for (1) and (2) so that the closed-loop system has a natural oscillation at velocity $v_o$ as a stable limit cycle.

The key idea in Problem A is to consider the "frozen system" (1) in which the locomotion velocity is a fixed constant $v(t) \equiv v_o$. The frozen system describes the linear dynamics governing the body shape change when the locomotor body is hypothetically forced to move at a constant velocity $v_o$ relative to the environment. For instance, a fish body in a fluid at flow speed $v_o$, with its center of mass pinned to the inertial frame, would be subject to the frozen system dynamics and may tend to have a decaying oscillation after a perturbation. We will define the natural oscillation as a periodic solution of the frozen system under an appropriate linear damping compensation to make the system marginally stable. The natural oscillation thus defined turns out to give body movements that are similar to those observed in biology and are useful for the design of locomotion control system.

The natural oscillation characterized by (1) with $v(t) \equiv v_o$ is not unique and can have an arbitrary amplitude since the frozen system is linear. We attribute an additional property to the definition of the natural oscillation to constrain the amplitude by (2) as follows. When a natural oscillation is imposed on the body, the locomotion velocity resulting through the dynamics (2) would oscillate around a constant value. In general, the average velocity is not equal to the value $v_o$ used in (1) to define the natural oscillation, leading to an inconsistency. We will use the freedom in the choice of the amplitude to meet the consistency requirement, and define the natural oscillation only for a particular value of the amplitude for which the resulting average velocity turns out to coincide with the original $v_o$. We will show how the amplitude can be chosen to enforce the consistency and make the average value of the velocity $v(t)$ equal to $v_o$.

For the control design in Problem B, we consider the state feedback case, where $\theta$, $\dot{\theta}$, and $v$ are assumed available for feedback. We will propose a simple nonlinear controller such that the body shape $\theta(t)$ locally orbitally converges to the natural oscillation at $v_o$, and the velocity $v(t)$ converges to a periodic signal with the average equal to $v_o$. The idea is to use feedback linearization on (1) first to replace $K(v)\theta$ with $K(v_o)\theta$ and obtain the frozen system, and then apply

a nonlinear feedback control to make $\theta(t)$ converge to the natural oscillation. As a result, the rectifier equation (2) defines a periodically time-varying linear system, and a rigorous analysis will be given for the periodicity and average value of solution $v(t)$.

The next two sections will address Problems A and B, respectively.

## III. Natural oscillations of asymmetric systems

Consider a locomotor progressing in a fixed direction at a constant velocity on average. The steady velocity of locomotion is maintained by the propulsive force resulting from the body shape change, interacting with the environment. We gain insights into the locomotion mechanism by reversing the cause/effect and asking the following: if the body is forced to move at a constant velocity $v$, would it naturally tend to oscillate? If so, such motion could be used as a definition for a natural oscillation. This motivates us to analyze stability of the oscillation equation (1) for a fixed, constant value $v_o$ of velocity, in which case the system becomes linear.

Recall that the natural oscillation of standard linear mechanical systems is a well established concept. In particular, a natural mode of oscillation is defined to be a free response of the modified system obtained by removing all the damping effects to achieve marginal stability for sustained oscillation. This definition is valid for the standard case where the stiffness and inertia matrices are symmetric positive (semi)definite. However, this idea does not directly apply to the locomotion system because simple removal of damping effects $D\dot\theta$ does not result in marginal stability of $J\ddot\theta + K(v_o)\theta = 0$ due to the asymmetry of $K(v_o)$. Hence, a new definition for natural oscillations is necessary.

Clearly, the system (1) is stable when the velocity is zero, provided $K(0)$ is symmetric positive definite as is the case for typical locomotion systems. By continuity, the frozen system (1) with $v(t) \equiv v_o$ would be stable for any value of $v_o$ smaller than a threshold, and oscillations, if any, would die out in the steady state. However, if the damping effect $D\dot\theta$ is gradually reduced, the oscillations may eventually become unstable. When the eigenvalues with the largest real part go across the imaginary axis, the system becomes marginally stable and the oscillations can be sustained. The natural oscillation can thus be defined as a free response of the modified system obtained by reducing the damping effect by an appropriate amount to achieve marginal stability for sustained oscillations. This basic idea and consistency consideration lead to the following.

**Definition 3.1:** *Consider the system described by (1) and (2) with Assumption 2.1. The periodic motion*

$$\vartheta(t) := \Re[ze^{j\omega t}] = Z\cos(\omega t + \phi), \quad Ze^{j\phi} := z, \qquad (3)$$

*is called a* natural oscillation *at velocity $v_o$ if the following two conditions hold:*

(i) *For $v(t) \equiv v_o$, the body shape $\theta(t)$ in (1) converges, for almost all initial conditions, to $a\vartheta(t+c)$ for some nonzero $a, c \in \mathbb{R}$, dependent on the initial condition, provided an appropriate damping compensation $u = \rho_o J\dot\theta$ is applied.*

(ii) *For $\theta(t) \equiv \vartheta(t)$, the velocity $v(t)$ in (2) converges to a periodic solution with average $v_o$ for all initial conditions.*

*The parameters $\omega$ and $z$ are referred to as the* natural frequency *and* mode shape *of the natural oscillation.*

Let us first consider condition (i) and find the appropriate value of the damping parameter $\rho_o$. In condition (i), the phrase "almost all" refers to the following property. The set of initial states, from which the convergence to $a\vartheta(t+c)$ does not occur, has zero volume in the state space. Consequently, for any initial condition, there exists an arbitrarily small perturbation that leads to the stated convergence property. When $v(t) \equiv v_o$, system (1) becomes linear, and the characteristic equation for (1) with $v(t) \equiv v_o$ and $u = \rho J\dot\theta$ is given by

$$(s^2 J + s(\mu - \rho)J + K(v_o))y = 0, \quad s \in \mathbb{C}, \quad y \in \mathbb{C}^n. \qquad (4)$$

Condition (i) holds if and only if the critical value $\rho = \rho_o$ is chosen so that the above equation has a pair of solutions $(s, y) = (j\omega, z)$ and $(-j\omega, \bar z)$, and all the other characteristic roots are in the open left half plane. In this case, $\theta(t)$ converges to $a\vartheta(t+c)$ for all initial conditions except for those that lie in the subspace orthogonal to the invariant subspace associated with eigenvalues $\pm j\omega$.

When $J$ and $K(v_o)$ are symmetric positive definite, condition (i), with "almost all" replaced by "some," provides the standard notion of natural oscillations, where the critical value of the damping parameter is given by $\rho_o := \mu$. In this case, the system is marginally stable with all the eigenvalues on the imaginary axis, defining multiple modes of natural oscillations. For the class of systems we consider, it is not obvious how to characterize the critical value $\rho_o$. The following result will provide a characterization of $\rho_o$ and explicitly state how the stability property changes with the value of $\rho$. Below, the set of eigenvalues of $M(v_o) := J^{-1}K(v_o)$ is denoted by $\mathbf{\Lambda}(v_o)$.

**Lemma 3.1:** *Let a real scalar $v_o$ be given and consider the system (1) with Assumption 2.1 satisfied. Denote the minimizer and the optimal value of*

$$\rho_o := \min_{\lambda \in \mathbf{\Lambda}(v_o)} \quad \mu + \frac{\Im(\lambda)}{\sqrt{\Re(\lambda)}}. \qquad (5)$$

*by $\lambda_o$ and $\rho_o$, respectively. Let $z$ be the eigenvector of $M(v_o)$ associated with eigenvalue $\lambda_o$, and define the periodic signal $\vartheta(t)$ by (3) with $\omega := \sqrt{\Re(\lambda_o)}$. Then, condition (i) of Definition 3.1 is satisfied. In particular, the system (1) with damping compensation $u = \rho J\dot\theta$, described by*

$$J\ddot\theta + (\mu - \rho)J\dot\theta + K(v_o)\theta = 0, \qquad (6)$$

*is exponentially stable if $\rho < \rho_o$, marginally stable if $\rho = \rho_o$, and exponentially unstable if $\rho > \rho_o$.*

In the above result, Assumption 2.1(b) allows for the simple characterization of the critical damping $\rho_o$. Assumption 2.1(c) guarantees that the minimization problem (5) is well posed and feasible. Assumption 2.1(d) guarantees that the minimizer of (5) is unique, which in turn implies that, when $\rho = \rho_o$, the system is marginally stable with a single pair of unrepeated eigenvalues on the imaginary axis. Consequently, for almost all initial conditions, the trajectory $\theta(t)$ converges to a periodic solution of the form $\theta(t) = a\vartheta(t + c)$, where $a, c \in \mathbb{R}$ are determined by the initial condition.

Next we consider condition (ii) in Definition 3.1, where $\vartheta(t)$ is constructed as described in Lemma 3.1. We first show that $v(t)$ in (2) globally converges to a periodic trajectory. When $\theta(t) \equiv \vartheta(t)$, the rectifier dynamics (2) defines a linear periodic

system with variable $v(t)$. Let us denote, with a slight abuse of notation, $\xi(\vartheta(t))$ and $\varphi(\vartheta(t), \dot{\vartheta}(t), \ddot{\vartheta}(t))$ by $\xi(t)$ and $\varphi(t)$, respectively, which are both periodic with period $T := 2\pi/\omega$. Noting that $\xi(t) > 0$ holds for all $t$, it can be verified that the trajectory $v(t)$ of the system (2) is always bounded. Since the system (2) is a linear $T$-periodic system with uniformly bounded solutions, it admits a $T$-periodic solution $\wp(t)$ (see Theorem 20.3, [54]). In fact, it can be verified using the standard linear system theory that the periodic solution is unique and admits the following explicit formula:

$$\wp(t) = \frac{1}{1 - e^{\bar{\xi} T}} \int_t^{t+T} e^{\int_t^\tau \xi(\sigma) d\sigma} \varphi(\tau) d\tau, \tag{7}$$

where $\bar{\xi}$ is the average value of $\xi(t)$ over one cycle. It is easy to see that the error $v(t) - \wp(t)$ satisfies

$$(\dot{v} - \dot{\wp}) + \xi(v - \wp) = 0, \tag{8}$$

which is a stable linear system due to $\xi(t) > 0$. As a result, every trajectory $v(t)$ of (2) globally converges to the periodic solution $\wp(t)$.

We now show how the consistency requirement $\bar{\wp} = v_o$ in condition (ii) can be satisfied, where $\bar{\wp}$ is the average value of $\wp(t)$ over one cycle. In particular, the magnitude of the eigenvector $z$, or the amplitude of $\vartheta(t)$, is not unique, and we use this freedom to satisfy condition (ii). The average $\bar{\wp}$ can be seen as a function of $v_o$ and $\alpha$, denoted by $\bar{\wp} = f(v_o, \alpha)$, where $\alpha := \|z\|$ is the oscillation amplitude, and $v_o$ is the velocity parameter used to define $\omega$ and $z/\alpha$ through the characteristic equation (4) with $\rho = \rho_o$. Then, condition (ii) is satisfied if $\alpha$ is chosen such that $v_o = f(v_o, \alpha)$. Summarizing the above development, we have the following.

**Theorem 3.1:** Let a real scalar $v_o$ be given and consider the system described by (1) and (2). Suppose Assumption 2.1 is satisfied. Define the function $f(v_o, \alpha)$ by the average value of the periodic signal $\wp(t)$ in (7) as described in the preceding paragraphs. Then there exists a natural oscillation at $v_o$ if and only if there exists a positive real scalar $\alpha$ such that $v_o = f(v_o, \alpha)$. In this case, a natural oscillation at $v_o$ is given by $\vartheta(t)$ in (3), where $\lambda_o$ is the minimizer of (5), $\omega$ is defined by $\omega := \sqrt{\Re(\lambda_o)}$, and $z$ is the eigenvector of $M(v_o)$ associated with eigenvalue $\lambda_o$, with the magnitude $\alpha := \|z\|$ chosen to satisfy $v_o = f(v_o, \alpha)$.

In general, the solution $\alpha$ to $v_o = f(v_o, \alpha)$ may not be unique, and there are $m$ natural oscillations at $v_o$ if there are $m$ solutions $\alpha$. In such case, the smallest $\alpha$ gives the natural oscillation that is the most efficient in the sense of achieving the given velocity $v_o$ with the smallest oscillation amplitude. It is difficult to solve $v_o = f(v_o, \alpha)$ for $\alpha$ analytically, but a numerical approach is feasible through a line search over $\alpha$ for each fixed value of $v_o$, computing the value $f(v_o, \alpha)$ as the average of the steady state velocity $v(t)$ obtained by simulating (2). If there is no solution $\alpha$, then the average velocity $v_o$ cannot be achieved by any natural oscillations (e.g., $v_o$ may be too large). For the control design, it would be more practical to fix the value of $\alpha$ so that the body motion has a reasonable amplitude, and plot the curve $\bar{\wp} = f(v, \alpha)$ on the $(v, \bar{\wp})$ plane for gridded points of $v$. The average locomotion velocity $v_o$ achieved by the natural oscillation with amplitude $\alpha$ can then be found by the intersection of the curve and the straight line $\bar{\wp} = v$. We will illustrate this idea later for a design example.

Computation of the function value $f(v_o, \alpha)$ involves numerical simulation and its repeated evaluation may take a long time for systems with many degrees of freedom. For such systems, an approximate but explicit formula for $f(v_o, \alpha)$ would be useful, which can be obtained as follows. First, assuming small amplitude $\|\theta\|$, the functions $\xi$ and $\varphi$ may be approximated through Taylor series expansions and truncation of higher order terms. When terms are retained up to the second order, the functions typically take the following form [40]:

$$\xi(\theta) = c + \theta^{\mathsf{T}} C \theta, \;\; \varphi(\theta, \dot{\theta}, \ddot{\theta}) = \dot{\theta}^{\mathsf{T}} S \dot{\theta} + \theta^{\mathsf{T}} S \ddot{\theta} + \dot{\theta}^{\mathsf{T}} Q \theta \tag{9}$$

for some scalar $c$ and square matrices $S$, $C$, and $Q$ such that $c > 0$ and $C = C^{\mathsf{T}} > 0$. In this case, it can readily be verified [55] through the averaging of (2) that the function $f(v_o, \alpha)$ is approximated by

$$\begin{aligned} \bar{f}(v_o, \alpha) &:= \frac{\omega \; \mathsf{z}^{\mathsf{T}} \mathsf{Q} \mathsf{z}}{\mathsf{z}^{\mathsf{T}} \mathsf{C} \mathsf{z} + 2c/\alpha^2}, \\ \mathsf{Q}_{ij} &:= Q_{ij} \sin(\phi_i - \phi_j) \\ \mathsf{C}_{ij} &:= C_{ij} \cos(\phi_i - \phi_j) \end{aligned}, \tag{10}$$

where $\omega$ and $z$ are defined for $v_o$ as in Theorem 3.1, $\phi_i$ is the phase angle of $z_i$, and $\mathsf{z}$ is the vector with the $i^{\text{th}}$ entry $|z_i|/\|z\|$. The parameters $\omega$, $\phi$, and $\mathsf{z}$ depend on $v_o$, but are independent of the amplitude $\alpha$. From the expression of $\bar{f}(v_o, \alpha)$ in (10), we see for a fixed value of $v_o$ that the average velocity $\bar{f}(v_o, \alpha)$ approaches zero as the amplitude $\alpha$ tends to zero, and that the magnitude of $\bar{f}(v_o, \alpha)$ is bounded and approaches a constant as $\alpha$ goes to infinity (but it should be kept in mind that the approximation $\bar{f} \cong f$ is valid when $\alpha$ is small). The boundedness of $\bar{f}$ shows that a large value of $v_o$ may not satisfy $v_o = \bar{f}(v_o, \alpha)$ for any $\alpha$, suggesting that natural oscillations with large amplitudes cannot achieve high speed locomotion. Note, however, that the bound on $\bar{f}$ is proportional to $\omega$, and hence a higher speed may be achieved by stiffening the body and increasing the natural frequency. This idea will be illustrated by an example later.

## IV. Entrainment to Natural Oscillation

We will develop a systematic method for designing a feedback controller for the system in (1) and (2) to achieve a natural oscillation at a prescribed velocity $v_o$. The control objective is precisely defined as follows.

**Definition 4.1:** *Consider the locomotion system described by (1) and (2) with the state vector $x := (\theta, \dot{\theta}, v) \in \mathbb{R}^{2n+1}$. Let $\vartheta$ in (3) be a natural oscillation at velocity $v_o$, and consider the velocity $\wp$ in (7) resulting from $\vartheta$. Define the periodic orbit in the state space*

$$\mathbb{O} := \{ \; \chi(t) \in \mathbb{R}^{2n+1} \mid t \in \mathbb{R} \; \}, \quad \chi := (\vartheta, \dot{\vartheta}, \wp). \tag{11}$$

*A feedback controller is said to achieve entrainment to the natural oscillation $\vartheta$ at $v_o$ if the trajectory $x$ converges to the orbit $\mathbb{O}$, i.e., there exists $t_o \in \mathbb{R}$, dependent upon the initial condition, such that*

$$\lim_{t \to \infty} \|x(t) - \chi(t + t_o)\| = 0$$

*holds for the closed-loop system whenever the initial value of $(\theta, \dot{\theta})$ is sufficiently close to the natural oscillation orbit*

$\mathbb{N} := \{\ (\vartheta(t), \dot{\vartheta}(t)) \mid t \in \mathbb{R}\ \}$, *i.e., the projection of the orbit* $\mathbb{O}$ *onto the* $(\theta, \dot{\theta})$ *subspace.*

The convergence requirement for the control design is local, as the design does not have to guarantee entrainment when the initial value of $(\theta, \dot{\theta})$ is not close to the orbit $\mathbb{N}$. However, the convergence should be guaranteed regardless of the initial value of $v$. To achieve entrainment to the natural oscillation $\vartheta$ at $v_o$, it suffices to make $\theta(t)$ converge to $\vartheta(t + t_o)$ for some $t_o$ because $v(t)$ converges to $\wp(t)$ when $\theta(t) \equiv \vartheta(t)$ as shown in the previous section. The average value of $\wp$ is equal to $v_o$ by definition since $\vartheta$ is a natural oscillation at $v_o$, thereby achieving locomotion at average velocity $v_o$. Thus, the control objective boils down to the convergence of $\theta(t)$ to $\vartheta(t + t_o)$. Our approach to the control design is based on two key ideas: feedback linearization and nonlinear damping compensation, which are explained next.

Recall that natural oscillations are defined for the frozen system where $v(t) \equiv v_o$ is assumed in (1). The frozen system defines linear dynamics in $\theta$ and can be obtained through feedback linearization by the control law of the form

$$u = w + K(v)\theta - K(v_o)\theta,$$

where $w$ is the auxiliary control input. The simplest way for achieving the natural oscillation is to compensate the damping by the controller $w = \rho J\dot{\theta}$. In this case, the closed-loop system is described by (6), and the choice $\rho = \rho_o$ makes $\vartheta$ a solution to (6) as stated in Lemma 3.1. However, this approach is not practical because the oscillation is critically sensitive to the parameter $\rho_o$ and the initial condition, lacking structural stability. For practical purposes, the controller should be designed to achieve the natural oscillation as (part of the) stable limit cycle $\chi$ of the closed-loop system as described in Definition 4.1. Since the frozen system is linear, the controller is necessarily nonlinear to create a structurally stable limit cycle. We consider the nonlinear damping augmentation by feedback control $w = \varepsilon J\dot{\theta}$, where $\varepsilon$ depends on the state $x$. We choose the $\varepsilon$ function so that $\varepsilon = \rho_o$ when $(\theta, \dot{\theta})$ is on the natural oscillation orbit $\mathbb{N}$, and $\varepsilon$ is appropriately adjusted when $(\theta, \dot{\theta})$ is perturbed away from $\mathbb{N}$.

**Theorem 4.1:** *Consider the system described by (1) and (2). Let a nonzero constant* $v_o$ *and the signal* $\vartheta$ *in (3) be given. Suppose Assumption 2.1 is satisfied, and* $\vartheta$ *is a natural oscillation at velocity* $v_o$*. Denote by* $\lambda_o$ *and* $\rho_o$ *the minimizer and the optimal value of (5). Then entrainment to the natural oscillation* $\vartheta$ *at* $v_o$ *is achieved by the controller*

$$u = \varepsilon(\|R^\dagger \dot{\theta}\|) J\dot{\theta} + K(v)\theta - K(v_o)\theta,$$
$$R^\dagger := 2 \begin{bmatrix} \Im(\ell) & \Re(\ell) \end{bmatrix}^\intercal, \tag{12}$$

*where* $\varepsilon : \mathbb{R} \to \mathbb{R}$ *is a continuously differentiable, strictly decreasing function such that* $\varepsilon(\omega) = \rho_o$*, and* $\ell$ *is the left eigenvector of* $M(v_o)$ *associated with the eigenvalue* $\lambda_o$*, normalized to satisfy* $\ell^* z = 1$.

Theorem 4.1 shows that, when the controller (12) is used to drive the system described by (1) and (2), the natural oscillation at velocity $v_o$ is achieved exactly, and the actual velocity $v(t)$ converges to a $T$-periodic signal in the steady state. Moreover, the average velocity approaches the prescribed constant value $v_o$. The controller (12) achieves and stabilizes the natural oscillation as part of the limit cycle $\chi$ of the closed-loop system by adjusting the amount of damping. The intuition behind the stabilization mechanism can be given in terms of the characteristic roots of (6) as follows. First, note that the natural oscillation can be described as

$$\vartheta(t) = R \begin{bmatrix} \cos\omega t \\ \sin\omega t \end{bmatrix}, \quad R := \begin{bmatrix} \Im(z) & \Re(z) \end{bmatrix}.$$

We then see that $\omega = \|R^\dagger \dot{\vartheta}\|$ since $R^\dagger$ is a pseudo inverse of $R$ such that $R^\dagger R = I$. On the natural oscillation orbit $\mathbb{N}$, we have $\rho = \varepsilon(\omega) = \rho_o$ and the characteristic equation (6) has a pair of roots $s = \pm j\omega$ on the imaginary axis and the other roots in the left half plane. It can readily be shown that the derivatives of real and imaginary parts of $s$ with respect to $\rho$ are both negative at $\rho = \rho_o$. Hence, if the frequency and amplitude are positively perturbed from the natural oscillation to make $\|R^\dagger \dot{\theta}\|$ larger, then the root $s = j\omega$ moves into the open left half plane with a reduced magnitude of the imaginary part. As a result, the frequency and amplitude tend to decrease and return to the values before the perturbation. A rigorous proof of convergence is given in the Appendix.

In general, the convergence would be faster if the slope of $\varepsilon(x)$ at $x = \omega$ is steeper, which can be explained as follows. Note that $s \in \mathbb{C}$ is a characteristic root of (6) if and only if

$$p(\lambda, s) := s^2 + (\mu - \rho)s + \lambda = 0, \tag{13}$$

holds for some generalized eigenvalue $\lambda$ of $(J, K(v_o))$. The pair $s = \pm j\omega$ satisfies (13) for $\lambda = \lambda_o$ and $\rho = \rho_o$. When the amplitude is positively perturbed from the natural oscillation, i.e., $\theta(t) = (1 + \delta)\vartheta(t)$ for $\delta > 0$, the damping compensation term $\rho$ becomes $\varepsilon(\|R^\dagger \dot{\theta}\|) = \varepsilon((1 + \delta)\omega) \approx \varepsilon(\omega) - r\delta\omega = \rho_o - r\delta\omega$ where $-r < 0$ is the slope of $\varepsilon(x)$ at $x = \omega$. The characteristic equation (13) with $\lambda = \lambda_o$ then reduces to

$$s^2 + (\mu - \rho_o + r\delta\omega)s + \omega^2 + j(\rho_o - \mu)\omega = 0$$

which has two solutions

$$\begin{aligned} s(\delta) \quad = \quad & -(\mu - \rho_o + r\delta\omega)/2 \\ & \pm\sqrt{(\mu - \rho_o + r\delta\omega)^2 - 4(\omega^2 + j(\rho_o - \mu)\omega)}/2 \end{aligned}$$

which depends continuously on $\delta$. For $\delta = 0$, one of the solutions is $j\omega$, defining the natural oscillation. The derivative of this solution with respect to $\delta$ is calculated as follows

$$\begin{aligned} \left.\frac{\partial s(\delta)}{\partial \delta}\right|_{\delta=0} \quad &= \quad -\frac{r\omega}{2} + \frac{(\mu - \rho_o)r\omega}{2(\mu - \rho_o + 2j\omega)} \\ &= \quad \frac{-2\omega^2 - j\omega(\mu - \rho_o)}{(\mu - \rho_o)^2 + 4\omega^2} r. \end{aligned}$$

As a result, the real part of $s(\delta)$ is approximately $-2\omega^2 r\delta/((\mu - \rho_o)^2 + 4\omega^2) < 0$, which characterizes a faster decay rate for a larger $r$, corresponding to a steeper slope of $\varepsilon(x)$ at $x = \omega$.

For locomotion systems during steady cruising, the velocity is not constant but fluctuates around a constant since the thrust generated by periodic body movements is not constant. Theorem 4.1 gurantees the average velocity $v_o$, but has no statement about velocity fluctuations. Let us consider a limiting case and gain insights into the size of fluctuations through the approximations in (9). The term $\xi(\theta)v$ in (2) represents the drag due to the environment force. We consider the case

$\xi(0) = 0$, or $c = 0$, which means that the drag experienced by the body at its nominal posture $\theta = 0$, is ignored. For instance, $\xi(0)v$ would be the fluid drag that needs to be overcome when towing an eel with its body straight at velocity $v$. In this limiting case, the approximate function $\bar{f}(v_o, \alpha)$ in (10) is independent of $\alpha$ since $c = 0$, suggesting that the amplitude $\alpha$ can be arbitrarily chosen in the control design. It can be shown that the magnitude of the velocity ripple is small when the oscillation amplitude $\alpha$ is small, i.e.,

$$\max_{0 \le t \le T} |\wp(t) - v_o| \to 0 \quad \text{as} \quad \alpha \to 0.$$

To see this, denote the Fourier series of the $T$-periodic signal $\wp(t)$ as follows:

$$\wp(t) = v_o + \sum_{k=1}^{\infty} c_k \cos \eta_k, \quad \eta_k := k\omega t + \gamma_k \tag{14}$$

for some $c_k, \gamma_k \in \mathbb{R}$, where the average value is $v_o$ by design. Substituting this $\wp$ into (2) as a solution $v = \wp$, we have

$$\sum_{k=1}^{\infty} (k\omega) c_k \sin \eta_k = \xi \left( v_o + \sum_{k=1}^{\infty} c_k \cos \eta_k \right) + \varphi.$$

Note that the magnitudes of $\xi$ and $\varphi$ in (9) with $c = 0$ approach zero as $\alpha$, the amplitude of $\theta$, goes to zero. Hence, in this limit, we have $c_k \to 0$ for all $k$ and thus the amplitude of fluctuation in $\wp(t)$ approaches zero. This analysis shows that the control design in Theorem 4.1 is reasonable in the sense that it can yield a small-amplitude natural oscillation with small velocity ripples when the nominal drag $\xi(0)$ is small.

## V. Application to a multi-link locomotor system

### A. Fliptail locomotor

As an example of the class of mechanical systems described by (1) and (2), we consider the "fliptail locomotor," a multi-segment system with a symmetric mechanical structure as shown in Fig. 1. Multiple links are connected by flexible joints to form two chains that are attached to the head. Each link is subject to environmental forces with directional preference [4]. We consider the case where the two chains undulate symmetrically about the $x$-axis so that the head moves along the $x$-axis without incurring displacements in the $y$-direction. Let $(x_o, y_o)$ be the coordinates of the head, and $v := \dot{x}_o$ be the head velocity resulting from the undulation. We assume that there are $n$ identical links in each chain, and each link has mass $m_o$, length $2l_o$ and moment of inertia $m_o l_o^2/3$, and each joint has torsional stiffness $k_o$. The angle between the $i^{\text{th}}$ link and the negative $x$-axis is denoted by $\theta_i$. Let $\tau_i$ be the torque applied at the $i^{\text{th}}$ joint. The environmental resistive force on each link is modeled as $f_n = \mu_n v_n$ and $f_t = \mu_t v_t$, where $f_n$ and $f_t$ are the force components in the direction tangent and normal to the link, $v_n$ and $v_t$ are the components, in the respective directions, of the velocity of the link gravity center, and $\mu_n$ and $\mu_t$ are proportionality constants [4].

The equations of motion are given by (1) and (2) with (see [4], [40] for the detailed derivation)

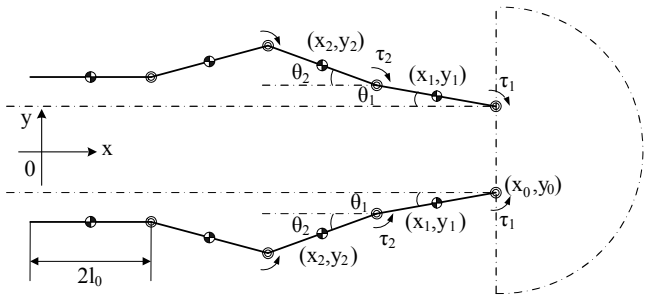


Fig. 1. The fliptail locomotor — a multi-segment system with symmetric mechanical structure moving along $x$-axis only.

$$c = \mu_t/m_o, \quad C = \mu_n I/m, \quad S = (l_o/n)\text{diag}(Fe),$$
$$Q = (l_o/m)((\mu_n - \mu_t)F + \mu_t S),$$

$$B = \begin{bmatrix} 1 & -1 & & \\ & \ddots & \ddots & \\ & & 1 & -1 \\ & & & 1 \end{bmatrix}, \; F = \begin{bmatrix} 1 & 2 & \cdots & 2 \\ & 1 & \ddots & \vdots \\ & & \ddots & 2 \\ & & & 1 \end{bmatrix},$$

$$J = m_o l_o^2 (FF^{\mathsf{T}} + I/3),$$
$$D = (\mu_n/m_o)J,$$
$$K = v\Lambda + k_o BB^{\mathsf{T}}, \quad u = B\tau,$$
$$\Lambda = l_o(\mu_n - \mu_t)F, \quad m = nm_o,$$

where $\xi(v)$ and $\varphi(v)$ are defined by (9), and $e \in \mathbb{R}^n$ is the vector with all its entries being one. We use the following parameter values unless otherwise noted: the number of links for each chain is $n = 5$, and each link has mass $m_o = 0.04$ kg and length $2l_o = 0.1$ m. The environmental force coefficients are $\mu_t = 0.01$ Ns/m and $\mu_n = 0.2$ Ns/m, and each joint has stiffness $k_o = 2.5 \times 10^{-4}\kappa$ Nm/rad, where the parameter $\kappa$ is used to examine the effect of stiffness perturbation. The system satisfies Assumption 2.1 for all $v_o \ge 0$.

### B. Natural oscillations

The profiles of natural oscillations are calculated for the fliptail locomotor for several cases of locomotion velocity $v_o$ and joint stiffness $k_o$ (parameterized by $\kappa$), and the result is summarized in Table I, where the natural oscillation is given by $\vartheta_i(t) = |z_i| \cos(\omega t + \phi_i)$ with $\omega$ equal to $2\pi$ divided by the period. For each case, the spectral decomposition of $M(v_o) := J^{-1}K(v_o)$ gives the eigenvalue $\lambda_o$ that solves the minimization problem in (5), the critical damping $\rho_o$, and the associated eigenvector $z$ of unit norm. The phase angles $\phi_i$ are given by those of the complex number $z_i$, and the natural frequency is calculated as $\omega = \sqrt{\Re[\lambda_o]}$. The oscillation amplitudes $|z_i|$ are given from $z_i := \alpha z_i$, where $\alpha$ is determined by the consistency condition $v_o = f(v_o, \alpha)$. Specifically, for various values of $\alpha$, the value $f(v_o, \alpha)$ is computed as the average of speed $v$ in the steady state when (2) is simulated with $\theta = \vartheta$. The plot of $f(v_o, \alpha)$ as a function of $\alpha$ is shown in Fig. 2 (left) for the case $\kappa = 5$ and $v_o = 0.3$ m/s. The function is monotonically increasing, and takes the

value 0.3 (dashed line) when the amplitude is $\alpha = 1.25$, which solves the consistency condition. The plots for the other cases are similar, and provide $\alpha = 0.45$ for the case $\kappa = 5$ and $v_o = 0.1$ m/s (Fig. 2, right), and $\alpha = 0.52$ for the case $\kappa = 1$ and $v_o = 0.1$ m/s. Note that the natural oscillation of the same system (with $\kappa = 5$) at a smaller velocity has a smaller amplitude as expected.

For each case, the phase of the $i^{\text{th}}$ joint angle $\phi_i$ lags behind its anterior neighbor $\phi_{i-1}$, indicating almost linearly decreasing phase from head to tail. This phase property results in traveling waves that propagate in the posterior direction, where the number of waves expressed by the fliptail at each time instant is roughly equal to $\phi_1/360$. We see that the amount of phase lag and the period of oscillation depend on $v_o$ and $k_o$. In particular, for a faster $v_o$ or a softer $k_o$, a body snapshot during locomotion exhibits more traveling waves. Figure 3 shows examples of body snapshots during natural oscillations at $v_o = 0.1$ m/s for soft ($\kappa = 1$) and stiff ($\kappa = 5$) cases.

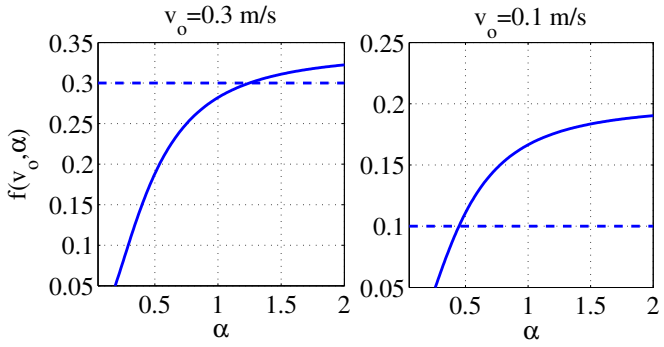


Fig. 2. Solution to $v_o = f(v_o, \alpha)$ for $v_o = 0.3$ m/s (left) and $v_o = 0.1$ m/s (right). The bold lines represent the function $f(v_o, \alpha)$ versus $\alpha$ and they intersect the dashed lines at $\alpha = 1.25$ and $\alpha = 0.45$, respectively.

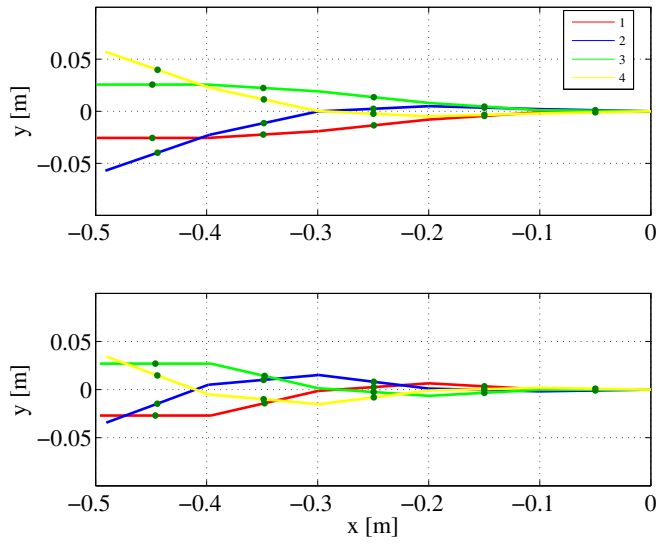


Fig. 3. Natural oscillation snapshots with different stiffness taken for every $1/4$ cycle in the order of $1, 2, 3, 4$. Above: $\kappa = 5$; Below: $\kappa = 1$.

### C. Control design for natural oscillation

Consider the fliptail locomotor with stiffness $\kappa = 5$. A controller is designed to achieve the natural oscillation at $v_o = 0.3$ m/s, using (12) with

$$\varepsilon(x) := \rho_o + \eta(\omega - x) \tag{15}$$

where $\eta$ is a constant design parameter. Choosing a positive value $\eta > 0$ makes the function $\varepsilon(x)$ monotonically decreasing, as required in Theorem 4.1. With $\eta = 2$ as an example, the closed-loop system is simulated with a random initial condition. As theoretically guaranteed, the profiles of simulated oscillations in the steady state almost exactly match the natural oscillation subject to numerical errors. The waveforms of the $\theta_i(t)$ oscillations are shown in Fig. 4, where the limit cycle trajectory achieved by the controller is purely sinusoidal. Figure 5 (top graph) shows that the specified velocity $v_o = 0.3$ m/s is exactly achieved on average.

Another controller is designed using $\eta = 0.2$ to achieve the same natural oscillation. The resulting performance is compared with that of the original controller with $\eta = 2$ to examine the effect of the design parameter. Figure 6 shows the asymptotic convergence of $\theta_1(t)$ for the two controllers. We see that the convergence is faster for $\eta = 2$ because the slope of $\varepsilon(x)$ at $x = \omega$ is steeper. Thus, the parameter $\eta$ can be tuned for faster convergence by making the slope steeper. A trade-off is that function $\varepsilon(x)$ with steep slope in a large range of $x$ would result in a control input with a large magnitude.

Yet another controller is designed to achieve a different natural oscillation, now at $v_o = 0.1$ m/s, with the same controller parameters $\eta = 2$. Figure 5 (bottom graph) shows that the specified average velocity $v_o = 0.1$ m/s is exactly achieved. Based on the discussion below Theorem 4.1, the ripples in $v(t)$ should get smaller as the oscillation amplitude approaches zero. Figure 5 shows the tendency consistent with this property; that is, the magnitude of the ripple is less for $\alpha = 0.45$ at $v_o = 0.1$ m/s than $\alpha = 1.25$ at $v_o = 0.3$ m/s.

In the above control designs, a particular average velocity $v_o$ is achieved by adjusting the amplitude of body oscillations, $\alpha$. As noted earlier, this method does not work when the velocity $v_o$ is large and no $\alpha$ satisfies the consistency condition $v_o = f(v_o, \alpha)$ due to boundedness of $f(v_o, \alpha)$. Also, the equations of motion, (1) and (2), are valid when the amplitude $\alpha$ is small, and hence if the solution $\alpha$ to the consistency condition is large, the velocity $v_o$ may not be achieved for the original fully nonlinear plant. In fact, biology of animal locomotion suggests that a larger velocity is achieved by increasing not amplitude but frequency [28]. This control strategy is actually in harmony with our natural oscillation framework. In particular, for a fixed oscillation amplitude $\alpha$, a desired locomotion velocity $v_o$ can be achieved by adjusting the stiffness, exploiting the fact that the nonzero solution $v_o$ to $v_o = f(v_o, \alpha)$ depends on the value of $\kappa$. Figure 7 shows plots of $y = f(x, \alpha)$ for several $\kappa$ values with $\alpha = 1.25$, where $v_o$ is identified from the intersection of a curve $y = f(x, \alpha)$ and the straight line $y = x$. We see that a larger stiffness leads to a larger velocity $v_o$ through increased oscillation frequency. The controller (12) can be modified by an additional term $k_c BB^{\mathsf{T}}\theta$ to adjust the closed-loop stiffness from $k_o$ to $k_o + k_c$. The additional term can be used to tune the

TABLE I
NATURAL OSCILLATION PROFILES ($\phi_5 = 0°$)

| $v_o$ (m/s) | $\kappa$ | Period (s) | $\phi_1$ | $\phi_2$ | $\phi_3$ | $\phi_4$ | $\|z_1\|$ | $\|z_2\|$ | $\|z_3\|$ | $\|z_4\|$ | $\|z_5\|$ |
|---|---|---|---|---|---|---|---|---|---|---|---|
| 0.3 | 5 | 1.22 | 267° | 190° | 115° | 49° | 2.5° | 8.1° | 21.5° | 34.6° | 58.3° |
| 0.1 | 5 | 2.21 | 155° | 112° | 66° | 16° | 1.3° | 4.3° | 7.0° | 13.5° | 20.1° |
| 0.1 | 1 | 2.12 | 352° | 246° | 151° | 69° | 1.0° | 3.9° | 9.3° | 15.9° | 23.2° |

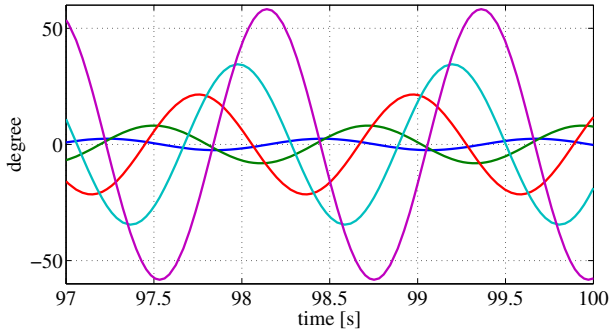


Fig. 4. The closed-loop oscillations are sinusoidal and match the natural oscillation profile in the first row of Table I.

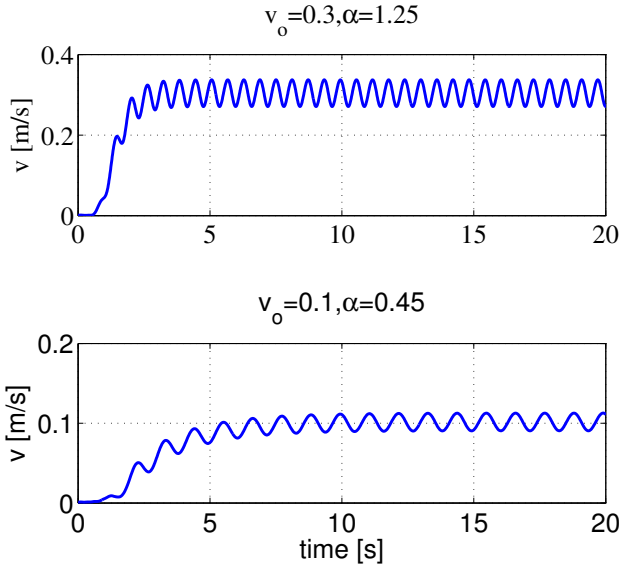


Fig. 5. Simulated velocity $v$. The target velocities $v_o = 0.3$ and $0.1$ m/s are achieved on average in the steady state, with smaller ripples for the latter.

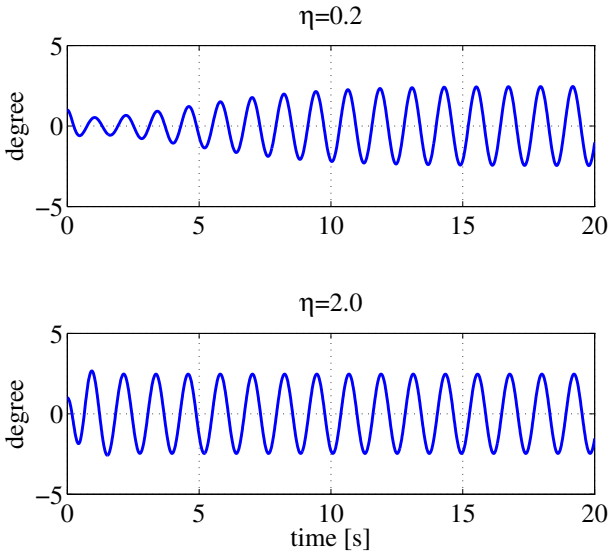


Fig. 6. Asymptotic convergence of $\theta_1(t)$ for different $\eta$.

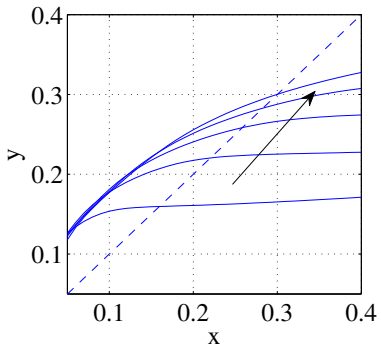


Fig. 7. Solution to $v_o = f(v_o, \alpha)$ with $\alpha = 1.25$ at various stiffness. The solid curves represent $y = f(x, \alpha)$ for $\kappa = 1, 2, 3, 4, 5$, along the arrow, and the dashed line is $y = x$. The intersection $x = f(x, \alpha)$ occurs at $x = 0.16, 0.22, 0.26, 0.28, 0.30$, respectively.

locomotion velocity of the system for set point tracking. This tracking scenario is demonstrated in Fig. 8 where $\kappa$ is changed via $k_c$ stepwise at $t = 100$ and 200 s to take values $3, 5, 1$ for successive durations. The closed-loop system exactly achieves the corresponding average velocities calculated in Fig. 7.

### *D. Accuracy of the bilinear model*

The proposed control design method is based on the approximate bilinear model of the locomotion system, (1) and (2), obtained by assuming small deformation of the body. It has been shown by multiple case studies [40] that the bilinear model captures the essential dynamics of locomotion and predicts optimal gaits that are reasonable for the original fully nonlinear model (before Taylor series truncation). Below, we examine whether the control design based on the approximate bilinear model is effective in the more realistic situation where the body deformation is not necessarily small.

We designed four controllers with four different values of the oscillation amplitude $\alpha$, and applied them to the fully nonlinear equations of motion (without bilinearization). To simplify the comparison, we consider the case with $\mu_t = 0$ such that the theoretical natural oscillation profiles are independent of $\alpha$. When the amplitude is small, the bilinear model captures the original nonlinear dynamics more accurately, and hence

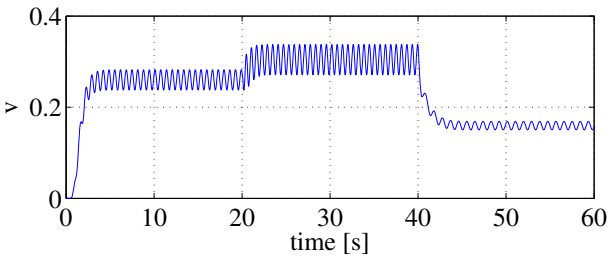


Fig. 8. Set point tracking of the velocity through $\kappa$.

the controller is expected to perform well in achieving the desired locomotion. This study reveals how much performance degradation occurs when the amplitude becomes larger. The simulation results are summarized in Table II. As expected, the natural oscillation is still effectively achieved when the oscillation angles are in a biologically reasonable range, e.g., $\alpha = 1.07$ rad in the table. When the oscillation amplitudes are further increased, one can observe significant distortion in oscillation profiles. If the error creates problems, an additional velocity feedback loop may be necessary.

## VI. Conclusion

We have considered a class of mechanical systems characterized by asymmetric stiffness matrices, arising from typical dynamics of animal locomotion. The natural oscillation is defined for such systems as a free response of damping-compensated systems, and is shown to capture rhythmic movements of e.g. flipping fish tails for swimming. Systematic methods are proposed for designing nonlinear feedback controllers to achieve entrainment to the natural oscillation exactly as a stable limit cycle. Also, the periodic movement of the body in a natural oscillation pattern induces a stable forward velocity and thus achieves an autonomous locomotion.

A standard method for the control of robotic locomotion systems would be a feedback regulation around a fixed periodic motion command (e.g. [4]). The design method proposed here is fundamentally different in that it achieves locomotion as a stable limit cycle of an autonomous closed-loop system. The pattern formation mechanism is thus inside the feedback loop, and our controller exploits natural dynamics of the system for efficient locomotion. Our theoretical result is based on an approximate model of the locomotor, which assumes that there are no external disturbances and the oscillation amplitude is small. The actual velocity of locomotion achieved by the proposed controller may be away from the target value if the assumption is violated. However, the proposed approach may be robust against modeling errors in generating the natural oscillation. Moreover, our controller may have potential capability of gait adaptation to changing environment. These robust/adaptive properties are expected due to the simple control mechanism of nonlinear damping compensation, leading to the natural oscillation associated with the given inertia and stiffness characteristics of the uncertain environment. Full experimental validation and theoretical justification of these properties are left for future research.

## Appendix

**Lemma 6.1:** *For any $\lambda \in \mathbb{C}$ with $\Re(\lambda) > 0$, the polynomial*

$$p(\lambda, s) := s^2 + cs + \lambda = 0,$$

*is Hurwitz (i.e., the solution $s$ has negative real part,) if and only if $c > |\Im(\lambda)|/\sqrt{\Re(\lambda)}$.*

*Proof:* The polynomial $p(\lambda, s)$ is Hurwitz if and only if the polynomial with real coefficients $q(s) := p(\lambda, s)p(\lambda^*, s)$ is Hurwitz. It is straightforward to verify using the Routh stability criterion that $q(s)$ is Hurwitz if and only if $c > |\Im(\lambda)|/\sqrt{\Re(\lambda)}$. ∎

**Proof of Lemma 3.1:** To show $\vartheta$ in (3) is a natural oscillation of (1) and (2), it suffices to prove that, for a specific value $\rho = \rho_o$, the characteristic roots $s$ of (6) are all in the open left half plane except for a complex conjugate pair on the imaginary axis. Note that $s \in \mathbb{C}$ is a characteristic root of (6) if and only if (13) holds for some eigenvalue $\lambda$ of $M(v_o)$. There are three cases to consider:

(i) $\lambda = \lambda_o$: The equation (13) with $\rho = \rho_o$ becomes $s^2 - (\Im(\lambda_o)/\sqrt{\Re(\lambda_o)})s + \lambda_o = 0$. It has two solutions $s = j\sqrt{\Re(\lambda_o)} = j\omega$ and $s = \Im(\lambda_o)/\sqrt{\Re(\lambda_o)} - j\sqrt{\Re(\lambda_o)}$ whose real part $\Im(\lambda_o)/\sqrt{\Re(\lambda_o)}$ is negative because $\lambda_o$ is the minimizer of (5).

(ii) $\lambda = \bar{\lambda}_o$: By the conjugate property, the equation (13) with $\rho = \rho_o$ has one solution $s = -j\omega$ and the other solution with negative real part.

(iii) $\lambda \neq \lambda_o$ and $\lambda \neq \bar{\lambda}_o$: By Lemma 6.1, the solution $s$ to the equation (13) with $\rho = \rho_o$ has negative real part if and only if $\mu - \rho_o > \Im(\lambda)/\sqrt{\Re(\lambda)}$, which is true because $\rho_o$ is the optimal value of (5).

What is left is to prove the stability properties, The system is stable if and only if the polynomial $p(\lambda, s)$ in (13) is Hurwitz for all $\lambda \in \mathbf{\Lambda}(v_o)$. By Lemma 6.1, for each $\lambda$, the polynomial $p(\lambda, s)$ is Hurwitz if and only if

$$\Re(\lambda) > 0, \quad \mu - |\Im(\lambda)|/\sqrt{\Re(\lambda)} > \rho.$$

This condition holds for all $\lambda \in \mathbf{\Lambda}(v_o)$ if and only if $\rho < \rho_o$ holds since $\Re(\lambda) > 0$ is implied by Assumption 2.1(c), and $\bar{\lambda} \in \mathbf{\Lambda}(v_o)$ if $\lambda \in \mathbf{\Lambda}(v_o)$. This proves the condition for exponential stability. The condition for exponential instability can be obtained by a similar argument using the Routh criterion. Finally, marginal stability condition follows by noting that only one pair of conjugate roots are on the imaginary axis when $\rho = \rho_o$ since $\rho_o$ is achieved in (5) by a unique minimizer. The system (6) is marginally stable with simple eigenvalues $\pm j\omega$ on the imaginary axis and the rest of eigenvalues are in the open left half plane when $\rho = \rho_o$. Hence, every trajectory converges to the natural oscillation at frequency $\omega$. ∎

**Proof of Theorem 4.1:** Let us use simplified notation where the dependence of parameters on $v_o$ is made implicit. For instance, $M(v_o)$ is denoted by $M$. The closed-loop system under consideration is

$$\ddot{\theta} + (\mu - \varepsilon(\|R^\dagger \dot{\theta}\|))\dot{\theta} + M\theta = 0. \tag{16}$$

Let matrices $N \in \mathbb{R}^{n\times(n-2)}$ and $N^\dagger \in \mathbb{R}^{(n-2)\times n}$ be such that

$$\begin{bmatrix} R^\dagger \\ N^\dagger \end{bmatrix} \begin{bmatrix} R & N \end{bmatrix} = I.$$

TABLE II
OSCILLATION PROFILES WITH DIFFERENT AMPLITUDES FOR THE ORIGINAL NONLINEAR MODEL ($\phi_5 = 0^\circ$)

| | Period (s) | $\phi_1$ | $\phi_2$ | $\phi_3$ | $\phi_4$ | $z_1$ | $z_2$ | $z_3$ | $z_4$ | $z_5$ | $\alpha$ (rad) |
|---|---|---|---|---|---|---|---|---|---|---|---|
| Theo. | 1.12 | 332° | 232° | 141° | 64° | 1.80° | 7.06° | 17.10° | 29.54° | 45.44° | 0.1/0.5/**1.0**/1.5 |
| Simu. | 1.12 | 333° | 235° | 143° | 65° | 1.79° | 7.03° | 17.12° | 29.54° | 45.43° | 0.10 |
| | 1.10 | 333° | 249° | 139° | 62° | 1.35° | 6.82° | 17.50° | 29.61° | 45.28° | 0.52 |
| | **1.10** | **344°** | **258°** | **128°** | **61°** | **1.21°** | **8.38°** | **19.4°** | **30.8°** | **43.39°** | **1.07** |
| | 1.23 | 327° | 209° | 116° | 53° | 4.74° | 11.23° | 24.17° | 31.8° | 39.24° | 1.44 |

Such matrices exist due to the assumption that the eigenvalues of $M$ are simple. In particular, the columns of $N$ (row of $N^\dagger$) can be the real and imaginary parts of the $(n-2)$ right (left) eigenvectors of $M$ corresponding to the eigenvalues other than $\lambda_o$ or $\lambda_o^*$. Under the new coordinates

$$\eta := \begin{bmatrix} \eta_1 \\ \eta_2 \end{bmatrix} := \begin{bmatrix} R^\dagger \\ N^\dagger \end{bmatrix} \theta, \qquad \begin{matrix} \eta_1 \in \mathbb{R}^2, \\ \eta_2 \in \mathbb{R}^{n-2}, \end{matrix}$$

the closed-loop system (16) becomes

$$\ddot\eta_1 + (\mu - \varepsilon(\|\dot\eta_1\|))\dot\eta_1 + R^\dagger MR\eta_1 = 0 \tag{17}$$
$$\ddot\eta_2 + (\mu - \varepsilon(\|\dot\eta_1\|))\dot\eta_2 + N^\dagger MN\eta_2 = 0, \tag{18}$$

where we noted $R^\dagger MN = 0$ and $N^\dagger MR = 0$.

For the subsystem (17), let us write $\eta_1$ in the polar coordinates:

$$\eta_1 = \xi \begin{bmatrix} \cos\varpi \\ \sin\varpi \end{bmatrix}$$

with the radius $\xi \in \mathbb{R}$ and the angle $\varpi \in \mathbb{R}$. Note that

$$v_1 := \begin{bmatrix} \cos\varpi \\ \sin\varpi \end{bmatrix}, \quad v_2 := \begin{bmatrix} -\sin\varpi \\ \cos\varpi \end{bmatrix}$$

$$\dot\eta_1 = \dot\xi v_1 + \xi v_2 \dot\varpi,$$

and hence, together with (17),

$$\begin{aligned} \ddot\eta_1 &= \ddot\xi v_1 + \dot\xi v_2\dot\varpi + \dot\xi v_2\dot\varpi - \xi v_1\dot\varpi^2 + \xi v_2\ddot\varpi \\ &= -(\mu - \varepsilon(\|\dot\eta_1\|))(\dot\xi v_1 + \xi v_2\dot\varpi) - R^\dagger MR\xi v_1. \end{aligned}$$

Multiplying $v_1^\intercal$ and $v_2^\intercal$ from left on the above equation gives the following two equations, (noting $v_1^\intercal v_2 = v_2^\intercal v_1 = 0$ and $v_1^\intercal v_1 = v_2^\intercal v_2 = 1$)

$$\begin{aligned} &\ddot\xi - (b/\omega)\dot\xi - \delta\dot\xi + \xi(\omega^2 - \dot\varpi^2) = 0, \\ &\ddot\varpi + 2(\dot\xi/\xi)\dot\varpi - (b/\omega)(\dot\varpi - \omega) - \delta\dot\varpi = 0. \end{aligned} \tag{19}$$

where $\delta := \varepsilon(\|\dot\eta_1\|) - \varepsilon(\omega)$ and the following facts are used:

$$\begin{aligned} R^\dagger MR = \begin{bmatrix} a & -b \\ b & a \end{bmatrix}, \quad & a = \Re(\lambda_o), \\ & b = \Im(\lambda_o), \\ v_1^\intercal R^\dagger MR v_1 = a = \omega^2, & \\ v_2^\intercal R^\dagger MR v_1 = b, \quad & \mu - \varepsilon(\omega) = -b/\omega. \end{aligned} \tag{20}$$

In (20), the last equation follows from $\varepsilon(\omega) = \rho_o = \mu + \Im(\lambda_o)/\sqrt{\Re(\lambda_o)} = \mu + b/\omega$.

We consider the system (19) as a three dimensional system with states $(\xi, \dot\xi, \dot\varpi)$. Obviously, the system has an equilibrium point $(\xi, \dot\xi, \dot\varpi) = (1, 0, \omega)$. Next, we will show this equilibrium point is asymptotically stable. To this end, we define $(\bar\xi, \dot{\bar\xi}, \dot{\bar\varpi}) = (\xi - 1, \dot\xi, \dot\varpi - \omega)$ and the linearized system at $(\bar\xi, \dot{\bar\xi}, \dot{\bar\varpi}) = (0, 0, 0)$ is

$$\begin{aligned} \ddot{\bar\xi} - g_1\dot{\bar\xi} - 2\dot{\bar\varpi}\omega = 0, \\ \ddot{\bar\varpi} + 2\omega\dot{\bar\xi} - g_1\dot{\bar\varpi} - g_2(\omega^2\bar\xi + \omega\dot{\bar\varpi}) = 0 \end{aligned} \tag{21}$$

where $g_1 = b/\omega < 0$, $g_2 := \varepsilon'(\omega) < 0$ and

$$\begin{aligned} \delta = \varepsilon(\|\dot\eta_1\|) - \varepsilon(\omega) \approx (1/\omega)\varepsilon'(\omega)\dot\eta_1^\intercal(\dot\eta_1 - v_2\omega) \\ = (1/\omega)\varepsilon'(\omega)(\dot\xi v_1 + \xi v_2\dot\varpi)^\intercal(\dot\xi v_1 + \xi v_2\dot\varpi - v_2\omega) \\ \approx \varepsilon'(\omega)(\dot{\bar\xi}\omega + \dot{\bar\varpi}). \end{aligned}$$

The characteristic equation for (21) is

$$a_3 s^3 + a_2 s^2 + a_1 s + a_0 = 0$$

with $a_3 = 1$, $a_2 = -(2g_1 + g_2\omega) > 0$, $a_1 = g_1^2 + g_1 g_2\omega + 4\omega^2$, and $a_0 = -2g_2\omega^3 > 0$. We can use the Routh table to verify that all the roots are in the open left half plane, and thus conclude stability of (21). In other words, we have $\lim_{t\to\infty}\dot\xi(t) = 1$ and $\lim_{t\to\infty}\dot{\bar\varpi}(t) = 0$ exponentially. The latter implies

$$\lim_{t\to\infty}\int_0^t \dot{\bar\varpi}(\tau)d\tau$$

exists, or equivalently, there exists a constant

$$\varpi_o := \lim_{t\to\infty}\Big(\varpi(t) - \omega t\Big).$$

As a result, we have

$$\lim_{t\to\infty}\eta_1(t) - \begin{bmatrix} \cos(\omega t + \varpi_o) \\ \sin(\omega t + \varpi_o) \end{bmatrix} = 0.$$

With $\xi = 1$ and $\varpi(t) = \omega t + \varpi_o$, we have $\|\dot\eta_1\| = \omega$, and hence

$$\mu - \varepsilon(\|\dot\eta_1\|) = \mu - \varepsilon(\omega) = -b/\omega$$

as shown in (20). As a result, the lower subsystem (18) becomes

$$\ddot\eta_2 - (b/\omega)\dot\eta_2 + N^\dagger MN\eta_2 = 0$$

which has the following characteristic equation

$$\det(s^2 I - (b/\omega)sI + N^\dagger MN) = 0. \tag{22}$$

Let $\mathbb{A}$ be the set of eigenvalues of $M$ other than $\lambda_o$ and $\lambda_o^*$. Because $N$ is spanned by the $n-2$ eigenvectors of $M$ associated with $\mathbb{A}$, for each eigenvalue $\lambda \in \mathbb{A}$, there exists a vector $w$ such that $M(Nw) = \lambda(Nw)$, and hence, $N^\dagger MNw = \lambda N^\dagger Nw = \lambda w$. Thus, $\mathbb{A}$ coincides with the set of eigenvalues of $N^\dagger MN$. Accordingly, $s$ is a characteristic root of equation (22) if and only if it satisfies $s^2 - (b/\omega)s + \lambda = 0$ for some $\lambda \in \mathbb{A}$. From Lemma 6.1, the polynomial is Hurwitz since $\lambda_o$ is given by (5) and $b/\omega = \Im(\lambda_o)/\sqrt{\Re(\lambda_o)}$. As a result, we have $\lim_{t\to\infty}\eta_2(t) = 0$.

Let

$$\vartheta(t) = R \begin{bmatrix} \cos(\omega t) \\ \sin(\omega t) \end{bmatrix} = Z\sin(\omega t + \phi), \quad t_o = \varpi_o/\omega.$$

It now follows that

$$\lim_{t\to\infty} \theta(t) - \vartheta(t + t_o) = \lim_{t\to\infty} R\eta_1(t) + N\eta_2(t) - R \begin{bmatrix} \cos(\omega t + \varpi_o) \\ \sin(\omega t + \varpi_o) \end{bmatrix} = 0.$$

The proof for $\lim_{t\to\infty} \dot{\theta}(t) - \dot{\vartheta}(t + t_o) = 0$ is similar and hence omitted.

Finally, when $\theta(t) = \vartheta(t)$, the velocity $v(t)$ in (2) globally converges to the periodic solution $\wp(t)$ due to the stable error dynamics (8) as shown in Section III.

■

## REFERENCES


[1] S. Hirose. *Biologically Inspired Robots: Snake-Like Locomotors and Manipulators*. Oxford University Press, 1993.

[2] H. Kimura, S. Akiyama, and K. Sakurama. Realization of dynamic walking and running of the quadruped using neural oscillator. *Autonomous Robots*, 7:247–258, 1999.

[3] J.W. Grizzle, G. Abba, and F. Plestan. Asymptotically stable walking for biped robots: analysis via systems with impulse effects. *IEEE Trans. Auto. Contr.*, 46(1):51–64, 2001.

[4] M. Saito, M. Fukaya, and T. Iwasaki. Serpentine locomotion with robotic snake. *IEEE Control Systems Magazine*, 22(1):64–81, 2002.

[5] M. Srinivasan and A. Ruina. Computer optimization of a minimal biped model discovers walking and running. *Nature*, 439(7072):73–75, 2006.

[6] A.J. Ijspeert, A. Crepsi, D. Ryczko, and J.M. Cabelguen. From swimming to walking with a salamander robot driven by a spinal cord model. *Science*, 315(5817):1416–1420, 2007.

[7] S.J. Chung and M. Dorothy. Nurobiologically inspired control of engineered flapping flight. *J. Guid. Contr. Dyn.*, 33(2):440–453, 2010.

[8] K. Seo, S.J. Chung, and J.J.E. Slotine. Cpg-based control of a turtle-like underwater vehicle. *Auton. Robot*, 28:247–269, 2010.

[9] M. Hirsch and S. Smale. *Differential Equations, Dynamical Systems, and Linear Algebra*. Academic Press, 1974.

[10] H.K. Khalil. *Nonlinear Systems*. Prentice Hall, 1996.

[11] J. Murray. *Lectures on Nonlinear Differential Equation Models in Biology*. Oxford, 1977.

[12] J. Marsden and M. McCracken. *The Hopf bifurcation and its applications*. New York, Springer-Verlag, 1976.

[13] J. Guckenheimer and P. Holmes. *Nonlinear Oscillations, Dynamical Systems, and Bifurcations of Vector Fields*. Springer-Verlag, 1983.

[14] M. Farkas. *Periodic Motions*. Springer-Verlag, 1994.

[15] I.I. Blechman. *Synchronization of dynamical systems*. Science, 1971.

[16] G.B. Ermentrout and N. Kopell. Frequency plateaus in a chain of weakly coupled oscillators, I. *SIAM J. Math. Anal.*, 15(2):215–237, March 1984.

[17] F.C. Hoppensteadt and E.M. Izhikevich. *Weakly Connected Neural Networks*. Springer-Verlag, New York, 1997.

[18] E.M. Izhikevich. *Dynamical Systems in Neuroscience: The Geometry of Excitability and Bursting*. Cambridge, MA, The MIT Press, 2006.

[19] A. Blaquiere. *Nonlinear System Analysis*. Academic Press, New York, 1966.

[20] M. Vidyasagar. *Nonlinear Systems Analysis*. Prentice-Hall, 1978.

[21] W. Lohmiller and J.J.E. Slotine. On contraction analysis for non-linear systems. *Automatica*, 34(6):683–696, 1998.

[22] W. Wang and J.J.E. Slotine. On partial contraction analysis for coupled nonlinear oscillators. *Biol. Cyb.*, 92(1):38–53, 2005.

[23] Q.C. Pham and J.J. Slotine. Stable concurrent synchronization in dynamic system networks. *Neural Networks*, 20:62–77, 2007.

[24] A. Shiriaev, J.W. Perram, and C. Canudas de Wit. Constructive tool for orbital stabilization of underactuated nonlinear systems: Virtual constraints approach. *IEEE Trans. Auto. Contr.*, 50(8):1164–1176, 2005.

[25] A. Shiriaev, A. Robertsson, J. Perram, and A. Sandberg. Periodic motion planning for virtually constrained Euler-Lagrange systems. *Syst. Contr. Lett.*, 55:900–907, 2006.

[26] G.A. Cavagna, N.C. Heglund, and C.R. Taylor. Mechanical work in terrestrial locomotion: Two basic mechanisms for minimizing energy expenditure. *Am. J. Physiol.*, 233:R243–R261, 1977.

[27] J. Rose and J.G. Gamble. *Human Walking*. Lippincott Williams and Wilkins, 2003.

[28] S. Kohannim and T. Iwasaki. Analytical insights into optimality and resonance in fish swimming. *J. Royal Society Interface*, 11:20131073, 2014.

[29] A.L. Fradkov. Exploiting nonlinearity by feedback. *Physica D*, 128:159–168, 1999.

[30] N.G. Hatsopoulos. Coupling the neural and physical dynamics in rhythmic movements. *Neural Computation*, 8(3):567–581, 1996.

[31] M.M. Williamson. Neural control of rhythmic arm movements. *Neural Networks*, 11:1379–1394, 1998.

[32] B.W. Verdaasdonk, H.F. Koopman, and F.C. Van der Helm. Energy efficient and robust rhythmic limb movement by central pattern generators. *Neural Network*, 19(4):388–400, 2006.

[33] B.W. Verdaasdonk, H.F. Koopman, and F.C. Van der Helm. Resonance tuning in a neuro-musculo-skeletal model of the forearm. *Biological Cybernetics*, 96(2):165–180, 2007.

[34] T. Iwasaki and M. Zheng. Sensory feedback mechanism underlying entrainment of central pattern generator to mechanical resonance. *Biological Cybernetics*, 94(4):245–261, 2006.

[35] Y. Futakata and T. Iwasaki. Formal analysis of resonance entrainment by central pattern generator. *J. Math. Biol.*, 57(2):183–207, 2008.

[36] Y. Futakata and T. Iwasaki. Entrainment to natural oscillations via uncoupled central pattern generators. *IEEE Trans. Auto. Contr.*, 56(5):1075–1089, 2011.

[37] D. Efimov, A.L. Fradkov, and T. Iwasaki. Exciting multi-DOF systems by feedback resonance. *Automatica*, 49(6):1782–1789, 2013.

[38] T. Bliss, T. Iwasaki, and H. Bart-Smith. Resonance entrainment of tensegrity structures via CPG control. *Automatica*, 48(11):2791–2800, 2012.

[39] T. Bliss, J. Werly, T. Iwasaki, and H. Bart-Smith. Experimental validation of robust resonance entrainment for CPG-controlled tensegrity structures. *IEEE Trans. Contr. Sys. Tech.*, 21(3):666–678, 2012.

[40] J. Blair and T. Iwasaki. Optimal gaits for mechanical rectifier systems. *IEEE Trans. Auto. Contr.*, 56(1):59–71, 2011.

[41] J. Chen, W.O. Friesen, and T. Iwasaki. Mechanisms underlying rhythmic locomotion: Body-fluid interaction in undulatory swimming. *J. Exp. Biol.*, 214(4):561–574, 2011.

[42] A. Goswami, B. Espiau, and A. Keramane. Limit cycles in a passive compass gait biped and passivity-mimicking control laws. *Autonomous Robots*, 4(3):273–286, 1997.

[43] B. Klaassen and K. Paap. GMD-SNAKE2: a snake-like robot driven by wheels and a method for motion control. *Proc. IEEE Int. Conf. Robotics & Auto.*, 4:3014–3019, 1999.

[44] P. Prautsch, T. Mita, and T. Iwasaki. Analysis and control of a gait of snake robot. *Trans. IEEJ, Industry Appl Soc.*, 120-D(3):372–381, 2000.

[45] A. Crespi, A. Badertscher, A. Guignard, and A.J. Ijspeert. Amphibot I: an amphibious snake-like robot. *Robotics and Autonomous Systems*, 50:163–175, 2005.

[46] E. Westervelt, B. Morris, and K. Farrell. Analysis results and tools for the control of planar bipedal gaits using hybrid zero dynamics. *Autonomous Robots*, 23(2):131–145, 2007.

[47] Z. Chen and T. Iwasaki. Robust entrainment to natural oscillations of asymmetric systems arising from animal locomotion. *Proc. IEEE Conf. Dec. Contr.*, pages 2954–2959, 2009.

[48] Z. Chen, L. Zhu, and T. Iwasaki. Autonomous locomotion of multi-link mechanical systems via natural oscillation pattern. *IEEE Conf. Decision and Control*, 2010.

[49] L. Zhu, Z. Chen, and T. Iwasaki. Synthesis of controllers for exact entrainment to natural oscillation. *World Congress on Intelligent Control and Automation*, 2010.

[50] T. Iwasaki. Multivariable harmonic balance for central pattern generators. *Automatica*, 44(12):4061–4069, 2008. (DOI:10.1016/j.automatica.2008.05.024).

[51] S. Kohannim and T. Iwasaki. Resonance in fish swimming to minimize muscle tension. *SICB Annual Meeting*, page P1.205, 2013.

[52] X. Liu, T. Iwasaki, and F. Fish. Dynamic modeling and gait analysis of batoid swimming. *Proc. American Control Conference*, 2013.

[53] J. Chen, J. Tian, T. Iwasaki, and W.O. Friesen. Mechanisms underlying rhythmic locomotion: Dynamics of muscle activation. *J. Exp. Biol.*, 214(11):1955–1964, 2011.

[54] H. Amann. *Ordinary Differential Equations: An Introduction to Nonlinear Analysis*. Walter de Gruyter, 1990.

[55] R. Forch and T. Iwasaki. Control of underactuated undulatory locomotor exploiting anti-resonance: A case study. *Proc. American Control Conf.*, 2009.

**Zhiyong Chen** received the B.E. degree from the University of Science and Technology of China, and the M.Phil. and Ph.D. degrees from the Chinese University of Hong Kong, in 2000, 2002, and 2005 respectively. He worked as a Research Associate at the University of Virginia during 2005-2006. He is now an Associate Professor at the University of Newcastle, Australia. His research interests include nonlinear systems and control, biological systems, and multi-agent systems. He is an Associate Editor of IEEE Transactions on Automatic Control and IEEE Transactions on Cybernetics.

**Tetsuya Iwasaki** received his B.S. and M.S. degrees in Electrical and Electronic Engineering from the Tokyo Institute of Technology (Tokyo Tech) in 1987 and 1990, respectively, and his Ph.D. degree in Aeronautics and Astronautics from Purdue University in 1993. He held faculty positions at Tokyo Tech (1995-2000) and at the University of Virginia (2000-2009), before joining the UCLA faculty as Professor of Mechanical and Aerospace Engineering. Dr. Iwasaki's current research interests include biological control mechanisms underlying animal locomotion, nonlinear oscillators, and robust/optimal control theories and their applications to engineering systems. He has received CAREER Award from NSF, Pioneer Prize from SICE, George S. Axelby Outstanding Paper Award from IEEE, Rudolf Kalman Best Paper Award from ASME, and Steve Hsia Biomedical Paper Award at the 8th World Congress on Intelligent Control and Automation.He has served as associate editor of IEEE Transactions on Automatic Control and several other journals.

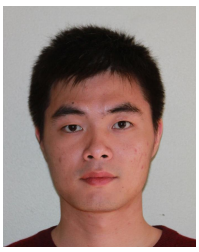

**Lijun Zhu** received the B.S. degree from the Xi'an Jiaotong University, Xi'an, China and the M.S. degree from Huazhong University of Science and Technology, Wuhan, China (both in mechanical engineering), in 2006 and 2008, respectively. In 2013, he received the Ph.D. degree in Electrical Engineering from University of Newcastle, Australia where he is currently working as a post-doc researcher. His research interests include dynamics and control of animal locomotion, robotics, and multi-agent systems.